Atmospheric Environment 173 (2018) 185–197

Contents lists available at ScienceDirect

Atmospheric Environment

journal homepage: www.elsevier.com/locate/atmosenv

Determination of chloromethane and dichloromethane in a tropical terrestrial mangrove forest in Brazil by measurements and modelling

S.R. Kolusu[a,c,*], K.H. Schlünzen[a], D. Grawe[a], R. Seifert[b]

[a] Meteorological Institute, CEN, University of Hamburg, Hamburg, Germany
[b] Institute for Geology and Marine Chemistry, University of Hamburg, Hamburg, Germany
[c] Department of Geography, School of Global Studies, University of Sussex, Brighton, UK

ARTICLE INFO

Keywords:
Chloromethane
Dichloromethane
Mangrove
Emission
METRAS

ABSTRACT

Chloromethane (CH_3Cl) and dichloromethane (CH_2Cl_2) are known to have both natural and anthropogenic sources to the atmosphere. From recent studies it is known that tropical and sub tropical plants are primary sources of CH_3Cl in the atmosphere. In order to quantify the biogenic emissions of CH_3Cl and CH_2Cl_2 from mangroves, field measurement were conducted in a tropical mangrove forest on the coast of Brazil. To the best of our knowledge these field measurements were the first of its kind conducted in the tropical mangrove ecosystem of Braganca. A mesoscale atmospheric model, MEsoscale TRAnsport and fluid (Stream) model (METRAS), was used to simulate passive tracers concentrations and to study the dependency of concentrations on type of emission function and meteorology. Model simulated concentrations were normalized using the observed field data. With the help of the mesoscale model results and the observed data the mangrove emissions were estimated at the local scale. By using this bottom-up approach the global emissions of CH_3Cl and CH_2Cl_2 from mangroves were quantified. The emission range obtained with different emission functions and different meteorology are 4–7 Gg yr^{-1} for CH_3Cl and 1–2 Gg yr_2 for CH_2Cl_2. Based on the present study the mangroves contribute 0.3 percent of CH_2Cl_2 and 0.2 percent of CH_3Cl in the global emission budget. This study corroborates the study by Manley et al. (2007) which estimated that mangroves produce 0.3 percent of CH_3Cl in the global emission budget. Although they contribute a small percentage in the global budget, their long lifetime enables them to contribute to the destruction of ozone in the stratosphere. From the detailed analyses of the model results it can be concluded that meteorology has a larger influence on the variability of concentrations than the temporal variability of the emission function.

1. Introduction

Atmospheric halocarbons such as chloromethane (CH_3Cl), bromomethane (CH_3Br) and dichloromethane (CH_2Cl_2) contribute to several atmospheric chemical processes (e.g. stratospheric ozone depletion). These halocarbons originate from both natural and anthropogenic sources such as biomass burning, incineration/industrial processes, oceanic emissions, coastal salt marshes and leaf litter (Khalil and Rasmussen, 1999; Lobert et al., 1999; Yokouchi et al., 2000b; Harper, 1985; Moore et al., 1996; Rhew et al., 2000; Blei et al., 2010; Kolusu et al., 2017). The quantification of halocarbons is uncertain. It is known that the global budgets of CH_3Cl and CH_3Br are imbalanced, i.e. known sinks are much larger than known sources (Butler, 2000; WMO, 2010). Field observations and modelling studies suggest that tropical and subtropical forest plants may be an important source of CH_3Cl (Yokouchi et al., 2000a,b; 2002; Lee-Taylor et al., 1998; Kolusu et al., 2017). Quantification of CH_3Cl and CH_2Cl_2 emissions from mangroves is relevant to the tropospheric ozone, since they contribute to its destruction. However, its major relevance is for climate studies, since CH_3Cl and CH_2Cl_2 have long atmospheric life time i.e. 1 year for CH_3Cl, 0.5 year for CH_2Cl_2 (WMO, 2010). This long life time is sufficient to transport and mix the halocarbons into the stratosphere and so impact atmospheric chemistry on the regional and global scale.

Our study estimates CH_3Cl and CH_2Cl_2 emissions from a mangrove forest region in tropical Braganca, Brazil. Mangroves forests are coastal forests found in sheltered estuaries and along river banks and lagoons in the tropics and subtropics. Mangrove forests are situated in sandy and muddy sheltered coastal locations (Hogarth, 1999). Mangroves are halophytic trees and woody shrubs that are exposed directly or indirectly to seawater halides. Their global range is approximated by the 20 °C winter ocean isotherm, and as such cover approximately 60–70% of the coastline between 25°N and S latitudes (Hogarth, 1999). Of the

* Corresponding author. Meteorological Institute, CEN, University of Hamburg, Hamburg, Germany.
E-mail address: s.kolusu@sussex.ac.uk (S.R. Kolusu).

https://doi.org/10.1016/j.atmosenv.2017.10.057
Received 11 August 2017; Received in revised form 18 October 2017; Accepted 24 October 2017
Available online 11 November 2017

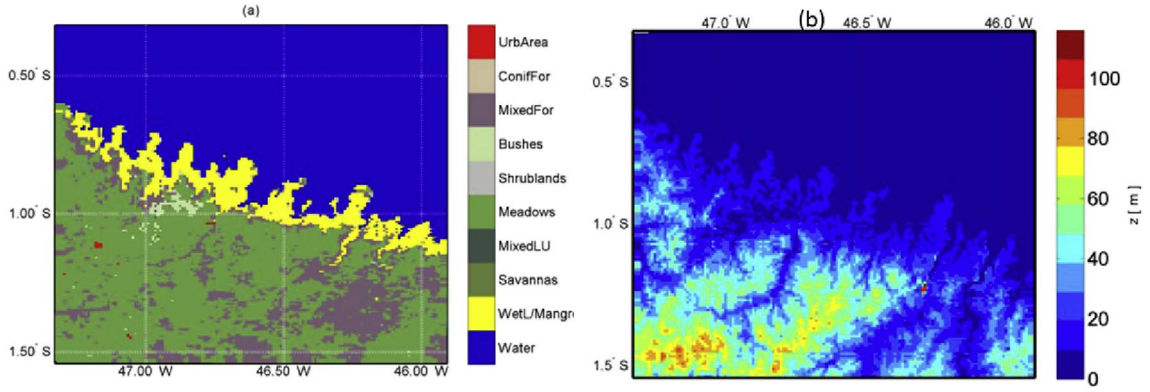

Fig. 1. Different landuse classes (a) and orography (b) of the model domain in the Brazil region.

50 to 75 recognized mangrove species, comprising 16–20 families, there are 4 major genera: Rhizophora, Avicennia, Bruguiera and Sonneratia (Ellison and Farnsworth, 2001; Hogarth, 1999; Kathiresan and Bingham, 2001). Mangrove forests support numerous ecosystem functions, including fisheries production and nutrient cycling. However, the areal extent of mangrove forests has declined by 30–50% over the past half century (Duke et al., 2007; Polidoro et al., 2010; Alongi, 2002). Current estimate of the global total area of mangroves using recently available Global Land Survey (GLS) and the Landsat archives is 137,760 km^2 (Giri et al., 2011).

Manley et al. (2007) studied the methyl halide emissions from greenhouse-grown mangroves. They estimated a global annual release of CH_3Cl from mangroves 12 Gg yr^{-1}. Kolusu et al. (2017) quantified emissions of CH_3Cl and CH_2Cl_2 over the tropical Atlantic Ocean and suggested tropical mangroves are possible source regions. Therefore, it is important to derive the CH_3Cl, CH_2Cl_2 emissions from mangroves. Quantified CH_3Cl and CH_2Cl_2 emissions from mangroves can be used in climate models to understand the impact of mangroves forest on the global atmospheric chemistry. Furthermore, since a change of mangroves can be expected due to sea level rise and global warming, it will be expected that the area of mangrove forests will also change globally in the future and thereby impacting emissions of CH_3Cl, CH_2Cl_2 into the atmosphere.

Hence, field measurements were conducted in the tropical Braganca mangroves forest region. The study region is located in the north eastern coastal part of Brazil, South America. The specific research questions addressed in this study are as follows: (1) Determination of CH_3Cl, CH_2Cl_2 emissions using observations and a mesoscale atmospheric model on the Braganca, Brazil from a mangrove forest. (2) What are the impacts of meteorology and different emission functions on the concentrations. The detailed description of data and method are presented in section 2. Section 3 presents the results, discussion and conclusions are given in section 4.

2. Method and data

2.1. Model description

The atmospheric MEsoscale TRAnsport and fluid (Stream) Model METRAS is adapted to simulate the meteorological conditions and transport of CH_3Cl, CH_2Cl_2 over the tropical region of Braganca, Brazil. METRAS is based on the primitive equations, ensuring the conservation of momentum, mass and energy. The three dimensional equations are solved in a terrain-following co-ordinate system. wind, temperature, humidity, cloud and rain water content as well as concentrations are derived from prognostic equations, whereas density and pressure are calculated from diagnostic equations (Schlünzen et al., 2012). METRAS has been used to simulate atmospheric phenomena in different regions and for different applications (Dierer et al., 2005; Lüpkes and Schlünzen, 1996; Niemeier and Schlünzen, 1993; Schlünzen and Katzfey, 2003). However, this is the first study where METRAS has been applied to the Braganca region.

The concentration of passive tracers are calculated in METRAS on an Eulerian grid by solving the equation for the conservation of mass in flux form:

$$\underbrace{\partial C/\partial t}_{a} = \underbrace{-\rho^{-1}\nabla(\rho\overline{C}\,\overline{v})}_{b} - \underbrace{\rho^{-1}\nabla(\rho\overline{C'v'})}_{c} + \underbrace{Q_{source}}_{d} + \underbrace{Q_{sink}}_{e} \quad (1)$$

Equation (1) gives the rate of change of the average concentration (a), the advection (b), turbulent diffusion (c), the sources (d) and the sinks (e). Chemical reactions and deposition of tracers are neglected in our study, because the chemical species have relatively long life times in the atmosphere about a year. Hence, in equation (1) the sink term (e) is neglected. A biogenic emission source has already been defined in METRAS for pollen emission (Schueler and Schlünzen, 2006). There are six different passive tracers defined in the model. Passive tracers are non-chemical reactions and only transport of concentrations. These tracers can be used for anthropogenic, biogenic or any other assigned emissions. Kolusu (2013) presented qualitative analyses of meteorology simulated by the model and details about type of passive tracers defined in the model which are used here to study the biogenic emissions in the Braganca region. Here we present the model results for constant and time dependent emission functions limited to the mangroves source region.

2.2. Model setup

The model domain is setup for the region of Braganca, Brazil. The Moderate Resolution Imaging Spectroradiometer (MODIS) land cover data are used, which have a horizontal resolution of 500 m. Shuttle Radar Topography Mission (SRTM) topography data of 100 m resolution are used for the model domain. Fig. 1 shows the different land-use classes and topography for the tropical region of Braganca, Brazil in METRAS. Meadows, mixed forest and mangroves are the most abundant land-use classes in the domain. The maximum orography height is about 115 m in the south west of the domain (Fig. 1b). The minimum orography height can be seen along the coastal Braganca region.

2.3. Meteorological data used for nudging

The High Resolution Brazilian Model (MBAR) is a Brazilian development of the High Resolution Model (HRM). MBAR forecasts of meteorological data of horizontal winds, potential temperature and specific humidity are used as forcing fields for METRAS. MBAR is a limited area, finite difference, hydrostatic, primitive equation high resolution regional model whose domain covers most of South America (http://www.inmet.gov.br/vime/). MBAR was developed by Deutscher Wetterdienst (DWD), the German Meteorological Service and was

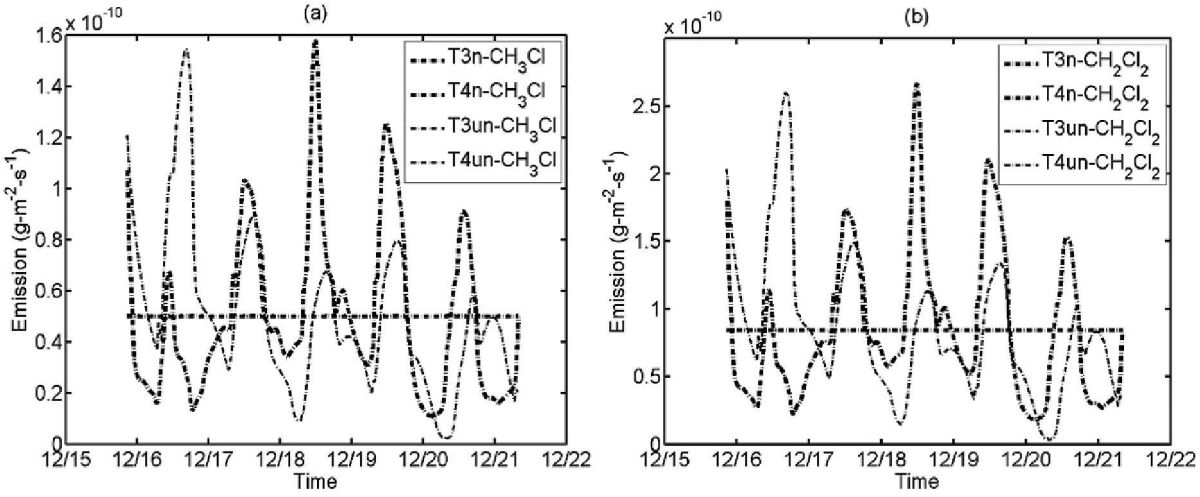

Fig. 2. Emission of chloromethane and dichloromethane for (a, b) mangrove forest source. T3n and T4n are for constant, time dependent emission function for nudge case.

implemented at the National Institute of Meteorology (INMET). MBAR needs initial and boundary conditions from a global model. DWD developed an operational global numerical weather prediction model, named German Global Model (GME), based on an almost uniform icosahedral-hexagonal grid. The MBAR model initial state and lateral boundary values are adapted from the analysis of GME. DWD provides the analyses and forecasts of GME on all 60 model levels and seven soil layers at a horizontal resolution of 30 km up to 78–120 h at 3-hourly intervals, based on the initial states for 00 and 12 UTC (Majewski et al., 2010).

The horizontal resolution of MBAR is 7 km. Hourly MBAR forecast data of wind, temperature and specific humidity are used as initial and lateral forcing for METRAS. The model METRAS has been run for about 6 days and 8 h. The model was run from 20:00 BRT, 15 December 2010, to 21 December 2010. The first day simulations will be considered for the spin up time of the model. The model METRAS has been setup for a Brazil domain with 1 km horizontal resolution. The model domain consists of 157 km by 174 km horizontal and 34 non-homogeneous vertical grid levels. In this simulation sea surface temperatures are obtained from the December 2010 mean of observation in the global ocean sea surface temperature data (HadISST1.1) developed by Rayner et al. (2003). The boundary conditions used in METRAS are as follows. For the lower boundary conditions of wind (u, v, w), fixed values (i.e. zero) were prescribed. Large-scale values are prescribed at the upper boundary using absorbing layers below. The lateral boundary conditions for the boundary normal wind components are calculated as far as possible from the prognostic equations, for the boundary parallel wind components a gradient of zero is assumed. Close to the lateral and upper boundaries a nudging term is added to the equations to ensure that wind, temperature and humidity can be nudged towards the forcing values of the coarser model (in this case MBAR).

The values of temperature and humidity are calculated from the energy budget equation at the lower model boundary. Zero gradients are used at the upper and lateral boundary for temperature and humidity. In the case of cloud water content, zero gradients were used at the lower and upper boundary. Large-scale values were prescribed as inflow points at the lateral boundary for cloud water content. For rain water content the flux at the boundary is set equal to the flux in the model at the lower boundary. The upper boundary conditions of rainwater content are zero gradients. At the lateral boundary, large-scale values are prescribed for rainwater content.

For the passive tracers at the lower boundary the flux at the boundary is calculated from a deposition velocity. However, this is set to zero in this study (see equation (1)). At the upper and lateral boundaries, zero gradients are used for the passive tracers. The boundary conditions are the same for all tracers.

2.4. Observations

Field work was carried out in December 2010. The experimental procedure follows the simple Lagrangian approach. In this method, the forest emission is calculated as the difference between the measured the concentration upwind and downwind of the forest. The site before the forest is called upwind. The site situated after the wind passed through the forest region is called downwind. Air samples were collected at upwind and downwind locations from the mangroves. The sample volume is 1L, a brief description of the configuration and validation of the sampling analysis for mixing ratios, isotopic determination is given by (Bahlmann et al., 2011), in which they have discussed the total sampling system. Samples were collected in Brazil and analysed in the laboratory by purge and trap gas chromatography with dry electrolytic conductivity detection (P&T-GCDELCD). However, only one day of quality assured samples for CH_3Cl and CH_2Cl_2 was valid from the field work due to problems in the sampling process. The concentartions of measured $CH_3Cl(CH_2Cl_2)$ at the downwind and upwind locations are 1451 pptv (216 pptv) and 707 pptv (38 pptv), respectively. The number of samples in this study is not expected to impact the derived emission functions due to the very long life time of the compounds in the atmosphere.

3. Results and discussion

METRAS has been run with a constant emission function and a time dependent emission function, which depends on humidity. The emissions simulated in METRAS for the mangrove source regions and emission functions are shown in Fig. 2. The time dependent emissions are liner correlated with relative humidity from pollen measurement data. We have assumed that the mangroves do react with temperature and humidity and applied the same relation for this study. We used these different emissions functions with different realization of meteorology to understand the role of these on concentration. For the mangrove source region, the time dependent emission functions of CH_3Cl (Fig. 2a) and CH_2Cl_2 (Fig. 2b), do show diurnal variation for METRAS (nudge) and METRAS (unnudge) meteorology case (denoted n or un). The constant emission functions are the same for the nudged meteorology case and unnudged meteorology case study. It can also be seen that emissions are higher during the daytime than the night-time as linearly correlated with humidity.

To quantify emissions, model studies are performed that are normalized with the measured data to achieve a reliable value for the

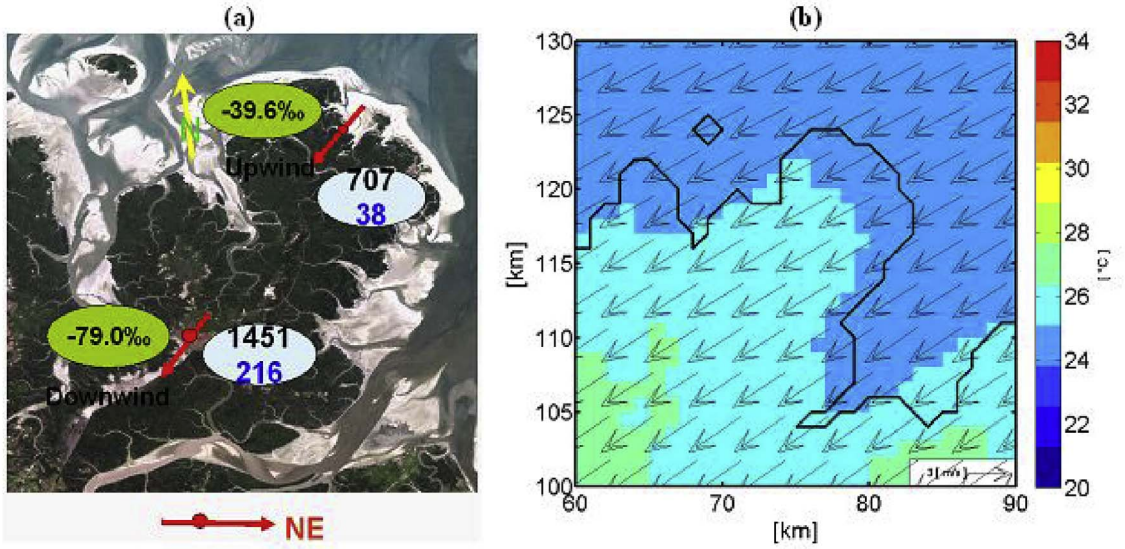

Fig. 3. Measured CH_3Cl concentrations(black), stable carbon isotope ratios (black) and CH_2Cl_2 (blue) concentrations (pptv) (a), meteorological conditions simulated with METRAS (b) for 17.12.2010 in the forest region. Every 3rd vector is shown. (For interpretation of the references to colour in this figure legend, the reader is referred to the web version of this article.)

emissions. However, measurements are rare and the commonly used method of a Lagrange approach is strictly valid only for homogeneous and stationary conditions. In the next section, we explain the scale factors derived from observations and models.

3.1. Scale factors for model emissions from observations

Different modelling studies have found that it is necessary to apply scaling factors to increase the aerosol emissions from sources to gain realistic mass concentrations (Kaiser et al., 2012; Marlier et al., 2013; Kolusu et al., 2015). Two emission functions are used: a constant emission function and a time dependent emission function where emission depends on humidity. The humidity-dependent emission function was originally obtained for pollen emissions and determined for the area of Lübeck by Schueler and Schlünzen (2006) but may be used for any passive (non–reactive) tracer. Both emission functions describe an assumed time dependence which even if it may not represent the true emission function can be used to study the possible impact of variable emission functions on concentrations. The magnitude of the emissions are scaled to achieve CH_3Cl and CH_2Cl_2 emissions using observational data.

The concentration increment due to emissions is linearly dependent on the emissions, if no chemical reactions or deposition takes place. For passive tracer dispersion this is not the case, therefore, the ratios between concentrations difference to emissions are constant.

Hence, the whole equation (2) can be normalized with the emissions, resulting in the following relation:

$$\Delta C/\Delta E = constant \tag{2}$$

The relation should not only hold for modelled results but also for measured data, thus for emissions based on the measured data one receives:

$$\Delta C_{Obs}/\Delta E_{Obs} = \Delta C_{Model}/\Delta E_{Model} \tag{3}$$

In equation (3) ΔC_{Obs} and ΔC_{Model} are the measured and modelled concentration gradients of CH_3Cl, CH_2Cl_2 during the observational time interval, respectively. ΔE_{Model} is the model emission of the source region in the simulation during the observational time interval. Therefore, the measurement based emission (named ΔE_{Obs} here) can be calculated as follows:

$$\Delta E_{Obs} = \Delta C_{Obs}.\ \Delta E_{Model}/\Delta C_{Model} \tag{4}$$

The ΔC_{Obs} is calculated as the concentration difference between upwind and downwind at the measurement sites. ΔC_{Model} is the model simulated concentration difference between upwind and downwind at the measurement sites. ΔE_{Model} is used for the corresponding measurement time interval for quantifying the CH_3Cl, CH_2Cl_2 emissions. In order to understand the impact of emission functions on concentration, the model concentrations were scaled such that the total emission (for the whole integration) for the time dependent emission function and constant emission function should be same. Based on this assumption scaling factors were calculated and these scaling factors (Kolusu, 2013) were then used to scale the simulated concentrations. Hence, one can compare, after normalization, the model simulated concentrations with different emission functions. In order to understand the role of meteorology on measured concentrations, two experiments were conducted with the mesoscale atmospheric model. The first experiment is METRAS, run without forcing, the second experiment is METRAS with forcing from MBAR data, both runs containing 6 different passive tracers (for different emission functions). Here, we presented the results for two tracers (T3,T4) for mangrove emissions.

Another uncertainty in the determination of emissions from concentrations is the form of the emission function. If emissions were merely constant with time, the measured concentrations might differ from those that were measured, such as with a time dependent emission function. However, the actual behaviour of the plants is more-or-less unknown. Therefore, both meteorological studies were performed for two types of emissions a constant one and a time dependent one.

3.2. Impact of meteorology on concentrations of CH_3Cl, CH_2Cl_2 in a coastal mangroves forest area

This study used the Lagrangian approach for measurement. The wind direction shows north easterly winds during the observations time. Fig. 3 gives the measured concentrations and model simulated meteorological conditions at the sampling time. Model simulated wind is mostly north easterly (Fig. 3b) before and after the sampling time. A wind shift could be observed at night-time only. Thus the selected upwind and downwind locations were more suitable for the air sample collections.

In air pollution studies the concentration changes are mainly dependent on the meteorological factors such as dispersion, transport and winds in the atmospheric boundary layer. The distinction between meteorological factors and emission functions is still incomplete, i.e. to which extent meteorlogy and emission functions impact on the

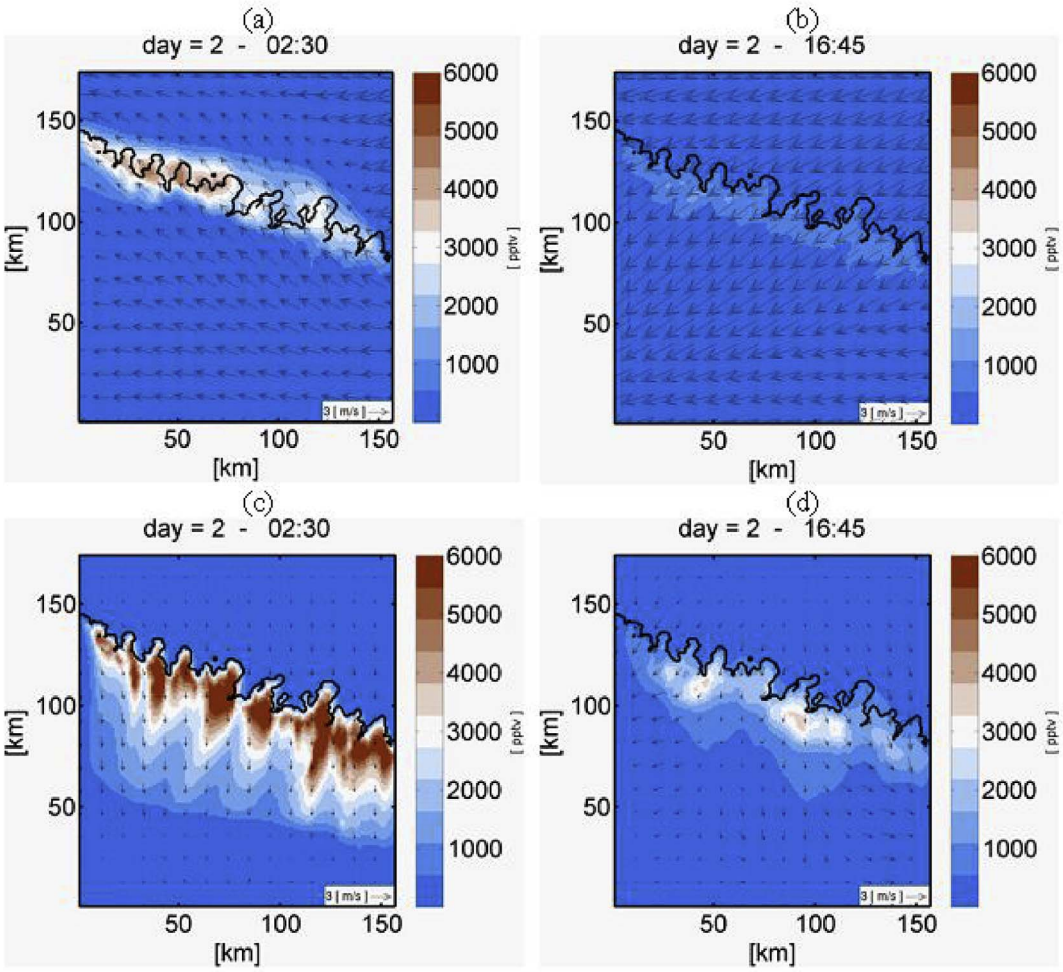

Fig. 4. CH_3Cl scaled concentrations and wind pattern at 20 m above the ground (a), (b) nudge meteorology case at night, day and (c), (d) unnudge meteorology case at night, day for 17.12.2010 with constant emission functions. Every 10th vector is shown.

concentration distribution. Hence, dispersion of passive tracers is studied using the mesoscale model METRAS with two different experiments. One is METRAS with forcing (nudge meteorology case) and METRAS without forcing (unnudge meteorology case). Fig. 4 shows the concentration transport during day (b, d) and night (a, c) time for the nudge and unnudge meteorology cases. The scaled concentrations of CH_3Cl (pptv) and CH_2Cl_2 (pptv) are shown in Figs. 4 and 5. Model simulated concentrations of the nudge meteorology case are in the range of the measurement data. The unnudge meteorology case concentrations are very high in comparison to the measurement due to large winds. The concentrations are transported with the model simulated wind flow. Higher concentrations at night can be seen in both the cases. It is also noted that higher concentrations occur in the unnudge meteorology case compared to the nudge meteorology case. This difference in concentration is due to the change in meteorology in both the cases.

Figs. 6 and 7 show the concentration gradient of CH_3Cl, CH_2Cl_2 in the mangrove forest region calculated from the model simulation. The gradient is calculated as the concentrations difference between downwind and upwind positions in the mangrove forest after scaling model concentrations, which is denoted as G in the Figures. This gradient gives the mangrove forest contribution of CH_3Cl, CH_2Cl_2. The diurnal cycle of CH_3Cl, CH_2Cl_2 gradients calculated from the nudge and unnudge meteorology case model simulations were studied to understand the impact of meteorology on the concentrations. The diurnal cycles of CH_3Cl, CH_2Cl_2 gradient vary similarly for both the tracers but the magnitude differs. The gradient of CH_3Cl, CH_2Cl_2 are slightly varying during nighttime in the nudge meteorology case. In the unnudge meteorology case, higher differences of the gradients are seen between the night and daytime. Higher difference in the gradient of CH_3Cl and CH_2Cl_2 is noticed on 17th, 18th, 19th, and 21st December 2010 in the unnudge meteorology case. These higher differences in the two different meteorology simulations suggest that meteorology is playing a role in the concentrations at the coastal mangrove forest on the constant emission functions. The ratio of gradient of CH3Cl and CH_2Cl_2 concentration for unnudge and nudge meteorology suggests that the unnudge meteorology case gradients are about 10 times higher than the nudge meteorology case except for the 21st December. On 21st December about 30 times higher concentration gradients are seen in the unnudge meteorology case for constant emission functions.

In order to determine the constant emission function from measurements, we need to have observations of CH_3Cl, CH_2Cl_2 continuously during the night and the daytime. Hence, it has been concluded that it is impossible to determine the constant emission functions using the limited measured data from the coastal mangroves forest, Brazil region. Although, our study aims to understand the impact of meteorology on the concentration distribution. In order to quantify the role of meteorology in concentrations, the concentrations simulated by METRAS were normalized using equation (5) for the constant emission function:

$$Norm.\ con. = \left(\frac{(T3un(z,x,y,t) - T3n(z,x,y,t)}{max(T3un(z,x,y,t);\ T3n(z,x,y,t))} \right) * 100 \quad (5)$$

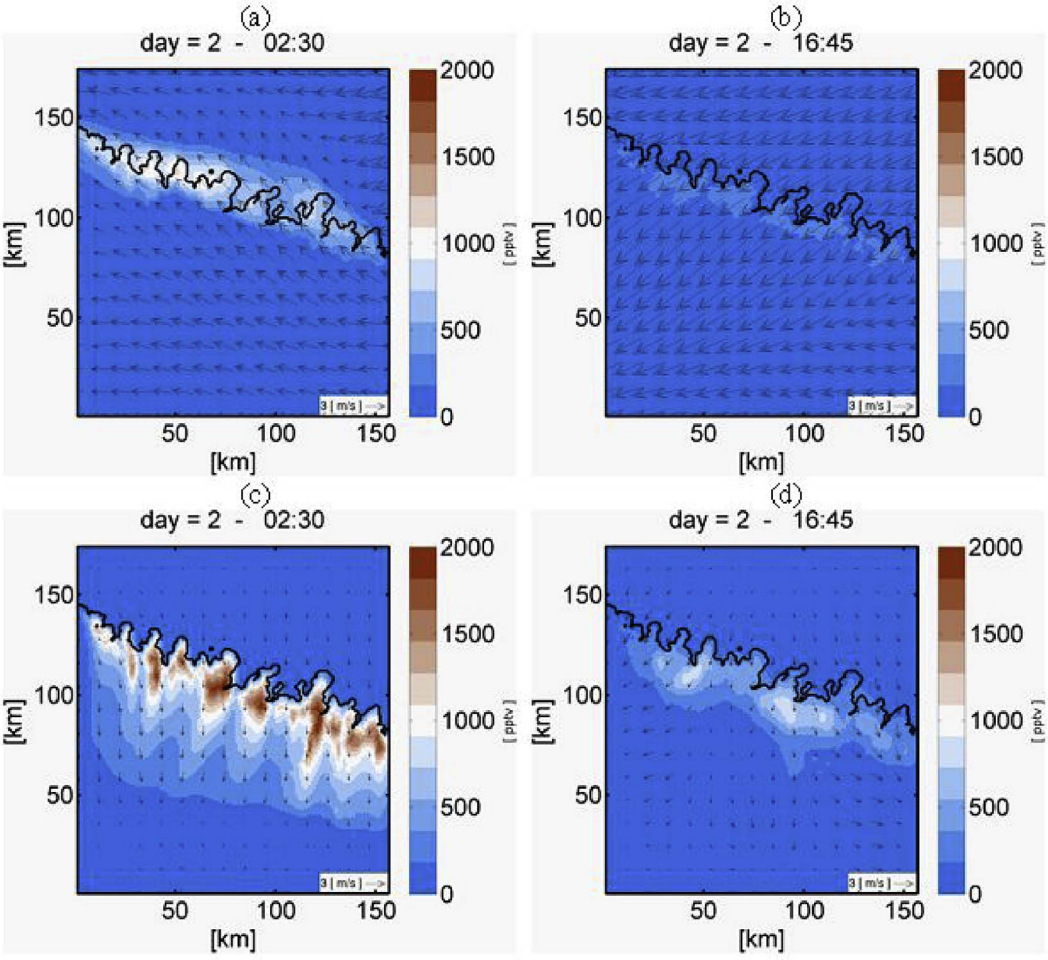

Fig. 5. CH_2Cl_2 scaled concentrations and wind pattern at 20 m above the ground (a), (b) nudge meteorology case at night, day and (c), (d) unnudge meteorology case at night, day for 17.12.2010 with constant emission functions. Every 10th vector is shown.

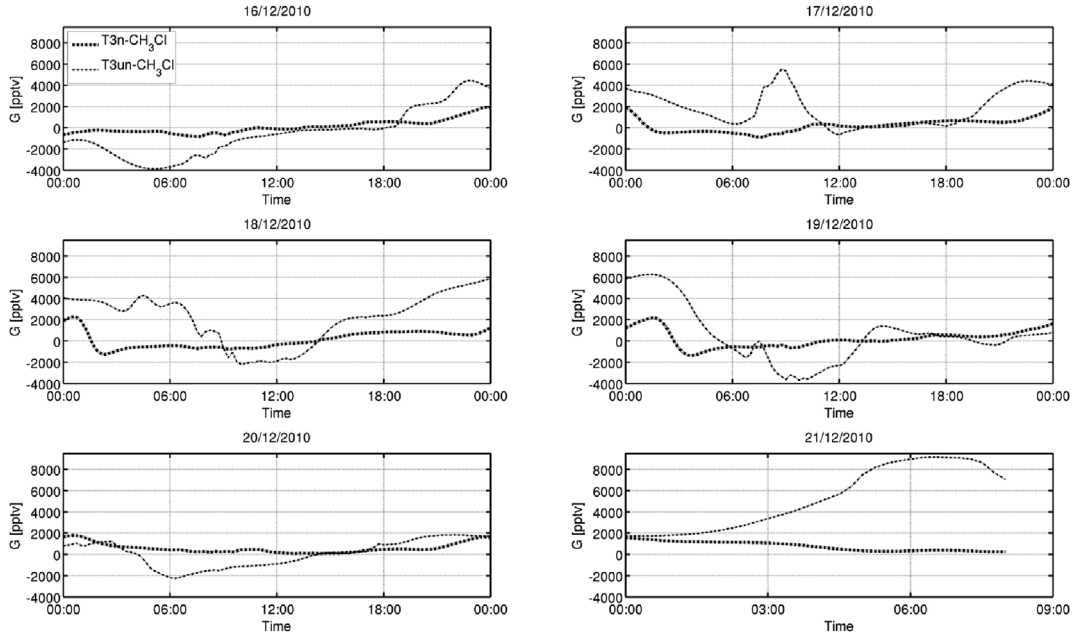

Fig. 6. Mangrove contribution of CH_3Cl constant emission functions for nudge (T3n), unnudge (T3un) meteorology case for different days. Note that 21.12.2010 is not for 24 h.

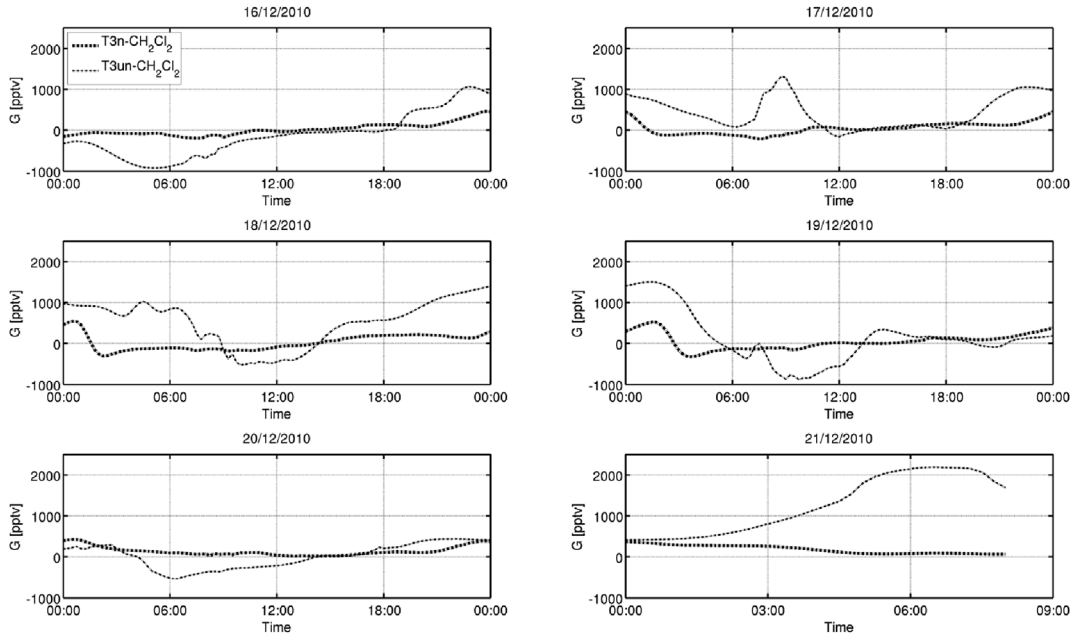

Fig. 7. Mangrove contribution of CH_2Cl_2 constant emission functions for nudge (T3n), unnudge (T3un) meteorology case for different days. Note that 21.12.2010 is not for 24 h.

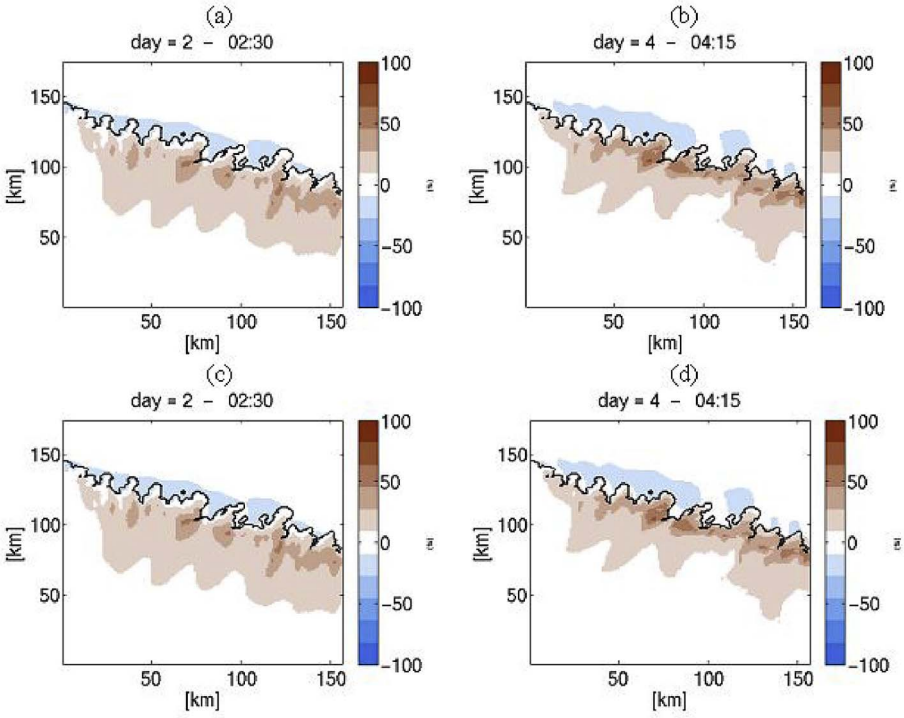

Fig. 8. Normalized concentrations difference of nudge and unnudge meteorology case for day 2 and day 4 for CH_3Cl (a, b) and for CH_2Cl_2 (c, d).

Here T3un(z,x,y,t) denotes the scaled concentration simulated by unnudge meteorology using constant emission function. Similarly, T3n (z,x,y,t) is for the nudge meteorology case.

Equation (5) is also used for the CH_2Cl_2 tracer. Fig. 8 shows the normalized concentrations of CH_3Cl, CH_2Cl_2 for 17.12.2010 (a, c) at 02:30 and for 19.12.2010 (b, d) at 4:15. The normalized concentration values are zero along the coast for a few hours about 9:00 to 12:00 and thereafter increased significantly on 20th December 2010 for CH_3Cl and CH_2Cl_2. The normalized concentrations of CH_3Cl, CH_2Cl_2 are in the magnitude of about +50% to −50% seen in the time series over the coastal mangrove region for most of the simulation. Hence, the quantified role of meteorology in the CH_3Cl and CH_2Cl_2 concentrations for constant emission function was about ± 50% in the mangrove forest region.

3.3. Impact of time dependent emission functions on concentrations

The scaled CH_3Cl and CH_2Cl_2 concentrations are shown in Figs. 9 and 10 for the nighttime and daytime. Like the concentrations emitted from the constant emission functions, concentrations simulated by the time dependent emission functions also show similar patterns in the nudge and unnudge meteorology case. Higher concentrations are seen for both tracers during the night due to stable stratification in the atmosphere. The stable stratification discourages vertical transport of the tracers in the atmosphere leading to an accumulation of emitted compounds. This stability impact is larger than the impacts of the increased

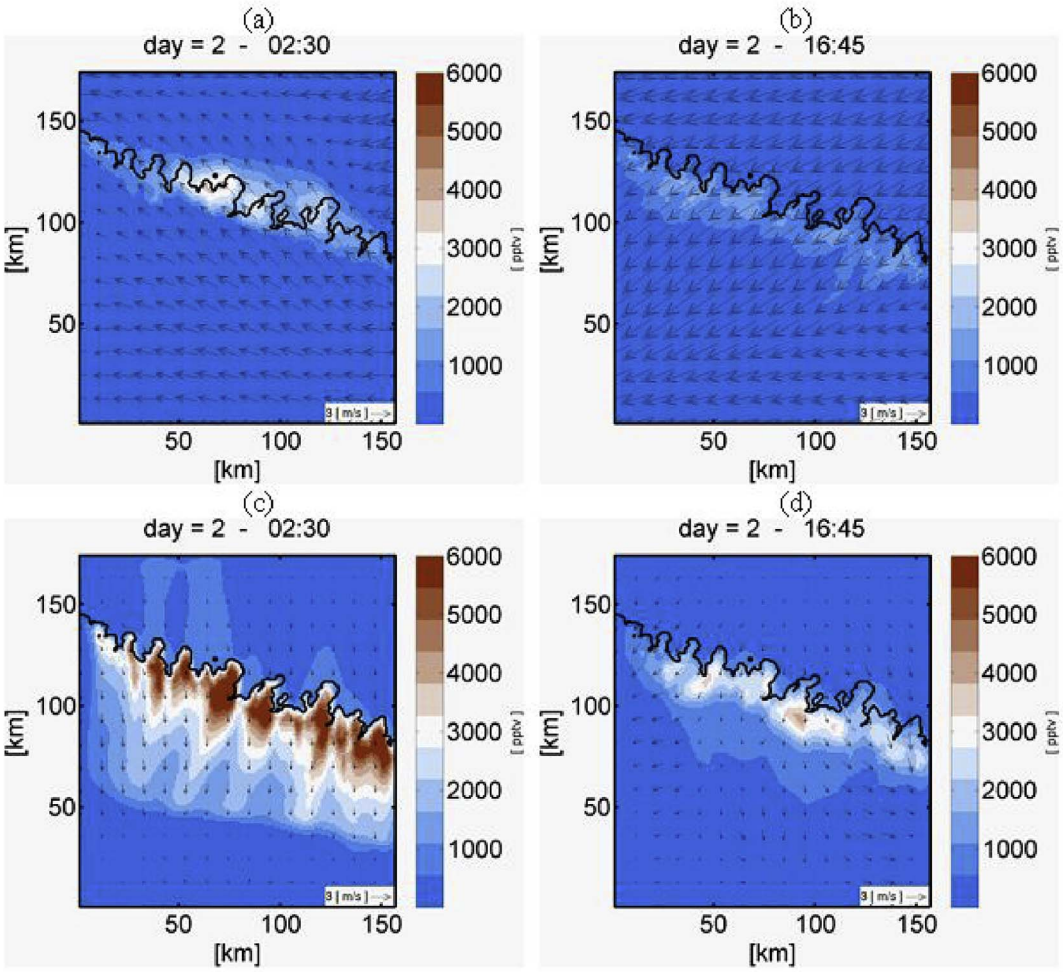

Fig. 9. CH_3Cl scaled concentrations and wind pattern at 20 m above the ground (a), (b) nudge meteorology case at night, day and (b), (d) unnudge meteorology case at night and day for 17.12.2010 with time dependent emission functions. Every 10^{th} vector is shown.

emissions during the daytime.

The magnitude of CH_3Cl and CH_2Cl_2 concentrations in the nudge meteorology case is within the observed data range. However, the magnitudes in the nudge meteorology case also vary substantially during the night with a magnitude about 3000 pptv due to meteorology changes. In the unnudge meteorology case the concentrations of CH_3Cl and CH_2Cl_2 are mostly trapped in the coastal mangrove region due to lower wind speeds simulated in the model. Unlike the unnudge meteorology case, the concentrations are more dispersed in the nudge meteorology case due to higher wind speed in the coastal mangrove region.

The diurnal cycle of concentration gradients of CH_3Cl is shown in Fig. 11. The concentration gradients of CH_3Cl are in the nudge meteorology case mostly constant during the day but slightly vary in the night. Unlike the nudge meteorology case the gradient of CH_3Cl diurnal cycle differ between night and day highly on 17th, 18th, 20th and 21st December in the unnudge meteorology case. There is a higher magnitude of gradient on 21st noted in the unnudge meteorology case, due to changes of the meteorology after 5 days simulations.

A similar pattern of diurnal variation of CH_3Cl (CH_2Cl_2 not shown) concentration gradients are found for the time dependent emission function and constant emission function in the nudge and unnudge meteorology cases. The only difference is the magnitude for both types of emission functions. This suggests that the type of emission functions likely does not have the largest impact on concentration. The ratios of CH_3Cl and CH_2Cl_2 concentration gradients from the unnudge meteorology case to the nudge meteorology case are: about 20 times on the 16th December; −10 to 10 times on the 17th.December; and slight variations are found on the 18th and 20th December 2010.

Equation (5) is also applied for the concentration simulated using time dependent emission functions also. Fig. 12 shows the normalized CH_3Cl (a, b) and CH_2Cl_2 concentration (c, d) for different days. The normalized model simulated concentrations of CH_3Cl, CH_2Cl_2 using time dependent emission functions are in the range of about ± 50 percent. Mostly, the normalized concentration calculated is +50 percent in the model whole simulations for CH_3Cl and CH_2Cl_2 in the coastal mangrove region. Hence, meteorology plays the same role on the concentrations given different types of emission functions.

3.4. Role of meteorlogy on constant and time dependency emission functions

To understand the role of both meteorology and time dependent emission functions, different combinations of frequency distributions were calculated. Such as one frequency distribution with different meteorology and constant emission functions. Another one with constant emission functions with different meteorology. Fig. 13 shows the differences in distribution of CH_3Cl (a, c) and CH_2Cl_2 (b, d). The x-axis denotes the concentration difference between unnudge and nudge meteorology case in pptv. The y-axes represent the number of grid points in percent. The total number of grid points was calculated as the product of total number of grid points in the south-north-direction (176), in the west-east-direction (159) and time (526 output intervals) at the 10 m model level.

Frequency distributions of CH_3Cl and CH_2Cl_2 show the distribution

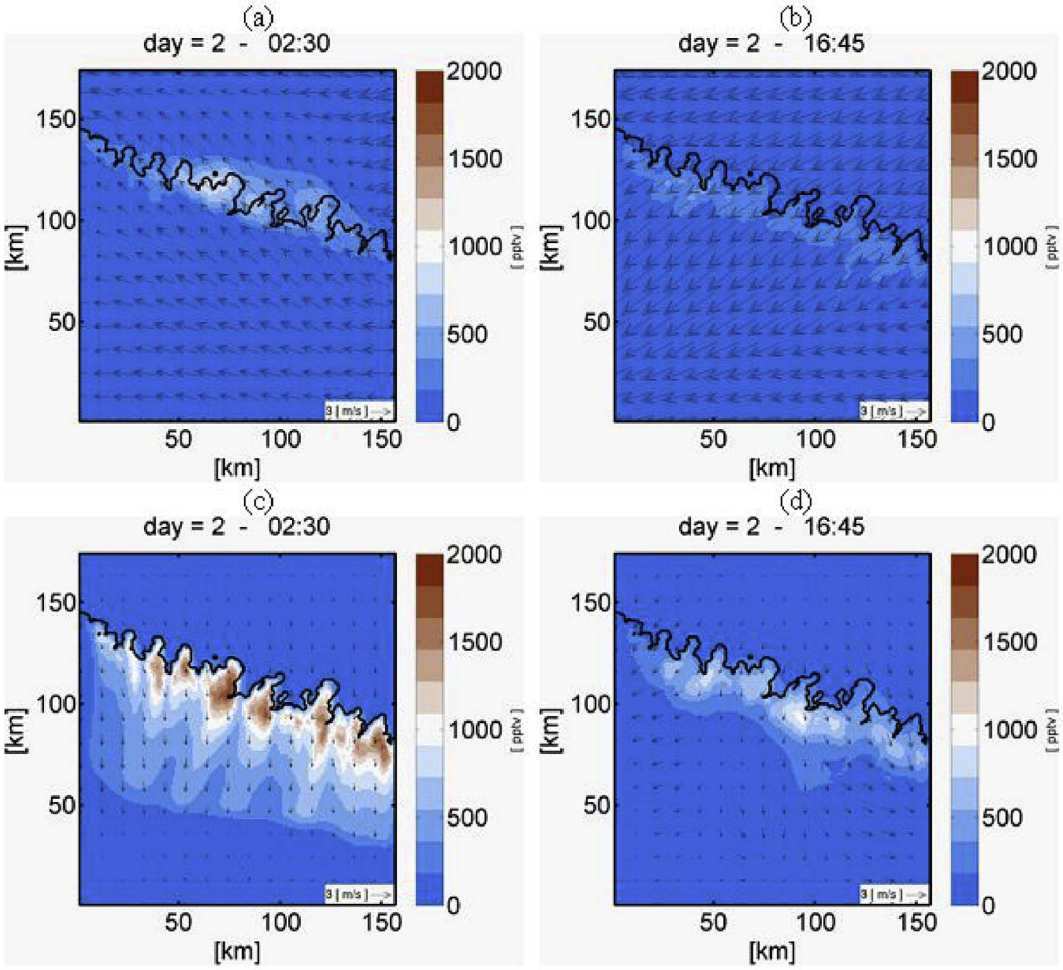

Fig. 10. CH_2Cl_2 scaled concentrations and wind pattern at 20 m above the ground (a), (b) nudge meteorology case at night, day and (b), (d) unnudge meteorology case at night, day for 17.1210 with time dependent emission functions. Every 10th vector is shown.

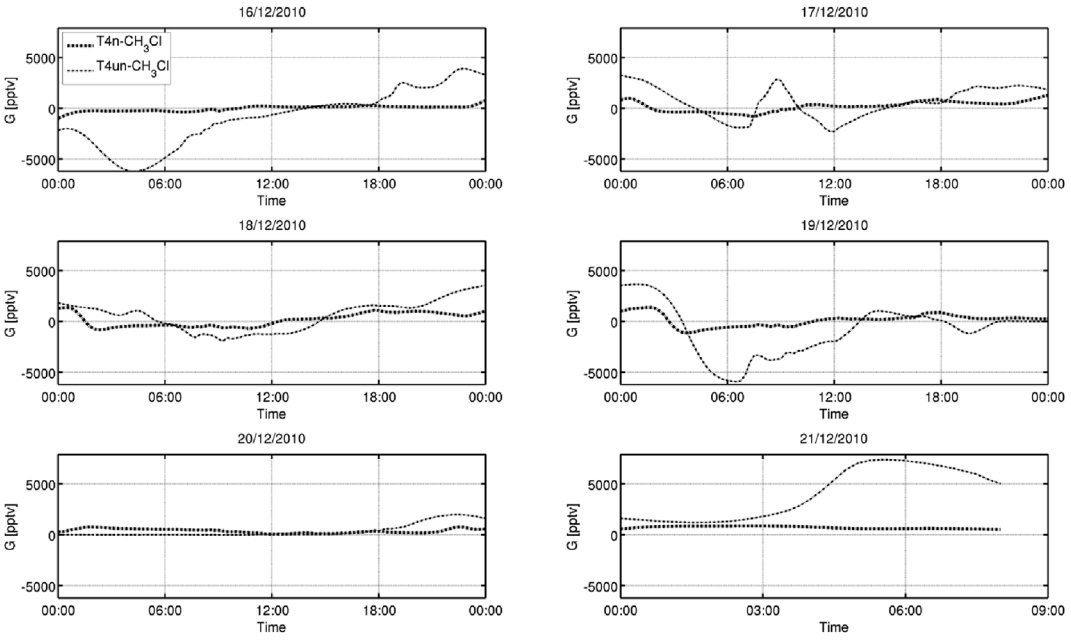

Fig. 11. Concentration gradients of CH_3Cl for time dependent emission function for different days. Note that 21.12.2010 is not for 24 h.

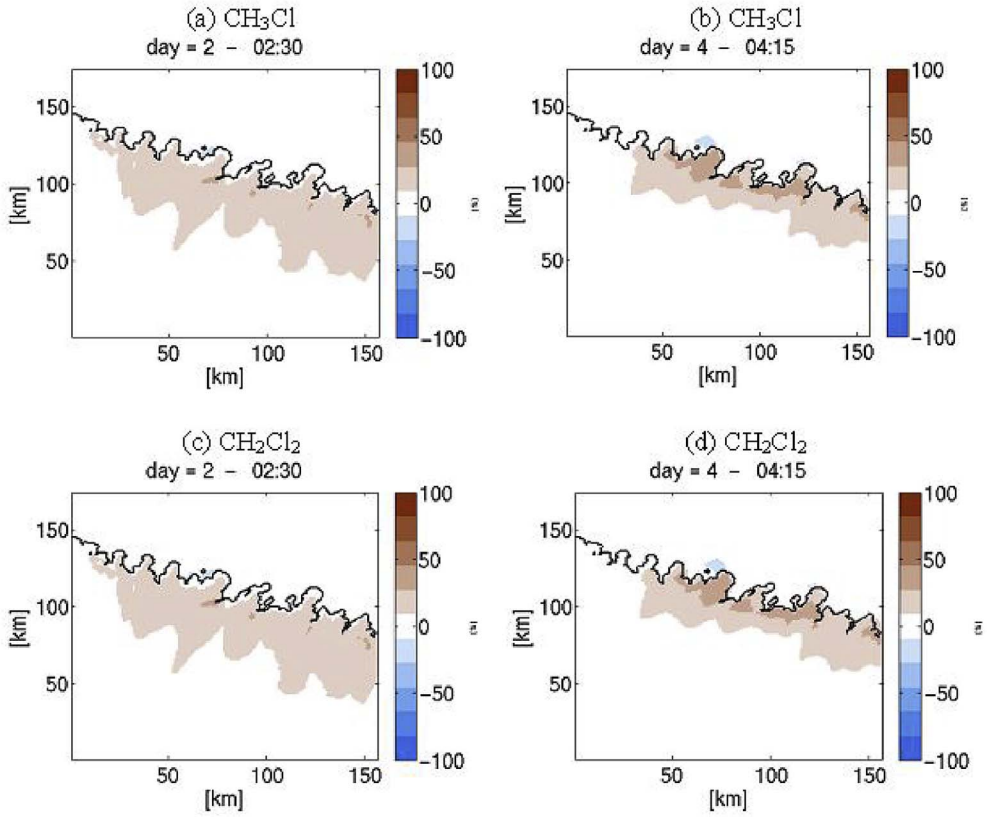

Fig. 12. Normalized concentrations difference of nudge and unnudge meteorology case for day 2 and day 4 for CH_3Cl (a, b) and for CH_2Cl_2 (c, d) for time dependent emission function concentrations.

is mostly positively skewed. More grid points show higher values in the unnudge meteorology case, so the concentrations are higher. The majority of grid points yield CH_3Cl concentration difference estimates within ± 2000 pptv for constant and time dependent emission functions. In the case of CH_2Cl_2 the concentration difference is about ± 1000 pptv. Thus, the frequency distribution plot suggests that the impact of meteorology on concentrations is high.

Similarly, the frequency distributions of the differences between

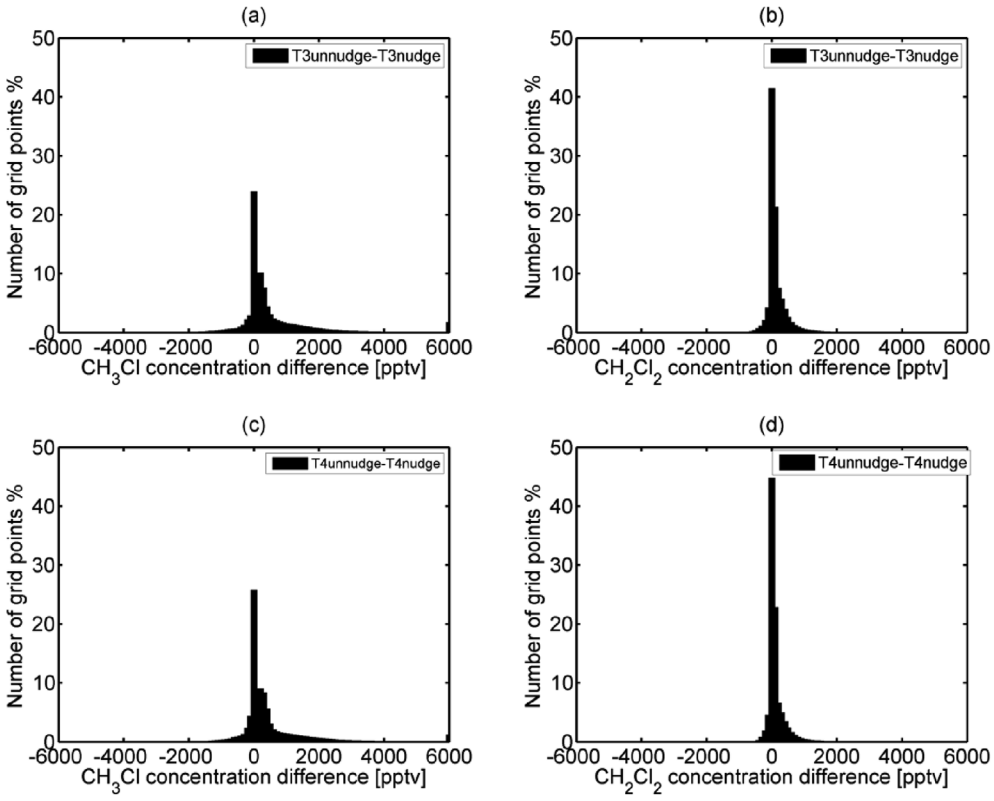

Fig. 13. Frequency distribution of CH_3Cl, CH_2Cl_2 for constant emission functions (a, b) and for time dependent emission functions (c, d).

Table 1
Percentiles of concentration difference of unnudge and nudge meteorology case for CH_3Cl and CH_2Cl_2 in pptv.

Percentiles	1	5	50	95	99
T3CH_3Cl	−1748	−598	204	3236	7528
T4CH_3Cl	−1165	−413	179	2830	6423
T3CH_2Cl_2	−418	−143	48	774	1801
T4CH_2Cl_2	−278	−98	42	677	1536

Table 2
Percentiles of concentration difference between different emission functions for CH_3Cl and CH_2Cl_2 in pptv.

Percentiles	1	5	50	95	99
T4n-T3nCH_3Cl	−2005	−788	−0.8	102	357
T4un-T3unCH_3Cl	−4000	−1300	0	303	112
T4n-T3nCH_2Cl_2	−479	−188	0	24	85
T4un-T3unCH_2Cl_2	−957	−311	0	72	266

concentration gradients of the nudge and unnudge meteorology cases were studied for the different emission functions. The frequency distribution of the differences in concentration gradients also reveals large differences due to meteorology changes (Figures not shown). The CH_3Cl concentration gradient difference extends from about −4500 pptv to 5000 pptv for constant and time dependent emission functions at the coastal mangrove region. In the case of CH_2Cl_2, the differences in concentration gradients are smaller, varying between −500 pptv to 1000 pptv for both types of emission functions. The wide distributions in the concentration gradient difference also support that meteorology has a large impact on the concentrations measureable over the coastal mangrove region.

Table 1 shows that the 1st, 5th, 50th, 95th, 99th percentiles of concentration differences (unnudge and nudge meteorology cases) of CH_3Cl, CH_2Cl_2 for the constant emission function (T3CH_3Cl, T3CH_2Cl_2) and for time dependent emission functions (T4CH_3Cl, T4CH_2Cl_2). Higher values of the 99th percentile of the data suggests that large differences in the concentrations are due to meteorology changes.

The analyses performed before by comparing results with the same emissions but different meteorology is now repeated for the same meteorology but different emission functions. Fig. 14 shows the frequency distribution of CH_3Cl, CH_2Cl_2 concentration difference of different emission function but same meteorology case. The frequency distribution shows that most of the grid points are in the 0 pptv concentration bin. Unlike in the different meteorology but same emission functions case, only few grid points show the concentration difference about less than 400 pptv in the constant meteorology but different emission function case. This suggests that the type of emission functions with same meteorology does not have more influence in the concentrations in the coastal mangrove region.

The same frequency distribution is also calculated for the gradient concentration differences. The gradient figures are not shown but reveal the same results for the mangrove emission of CH_3Cl, CH_2Cl_2.

The percentiles of concentration difference for constant meteorology but different emission functions is shown in Table 2. Table 2 supports the results of less difference in concentrations with the same meteorology. The 99th percentiles data of Table 1 is higher compared with data in Table 2. Hence, it has been concluded that, meteorology has shown more influence on the concentration than the little influence of different emission functions in the coastal mangrove region.

3.5. Determination of CH_3Cl and CH_2Cl_2 emissions from mangroves

Field measurements were conducted in the coastal mangrove forest in order contribute to the estimate of CH_3Cl and CH_2Cl_2 emissions from coastal mangrove forests. We employ a bottom-up approach in which detailed information about the small scale is aggregated and up-scaled to the larger scale. Therefore by determining the emission from a coastal mangrove forest we can extrapolate the local measurements to the global scale by multiplying the unit area flux with an estimated

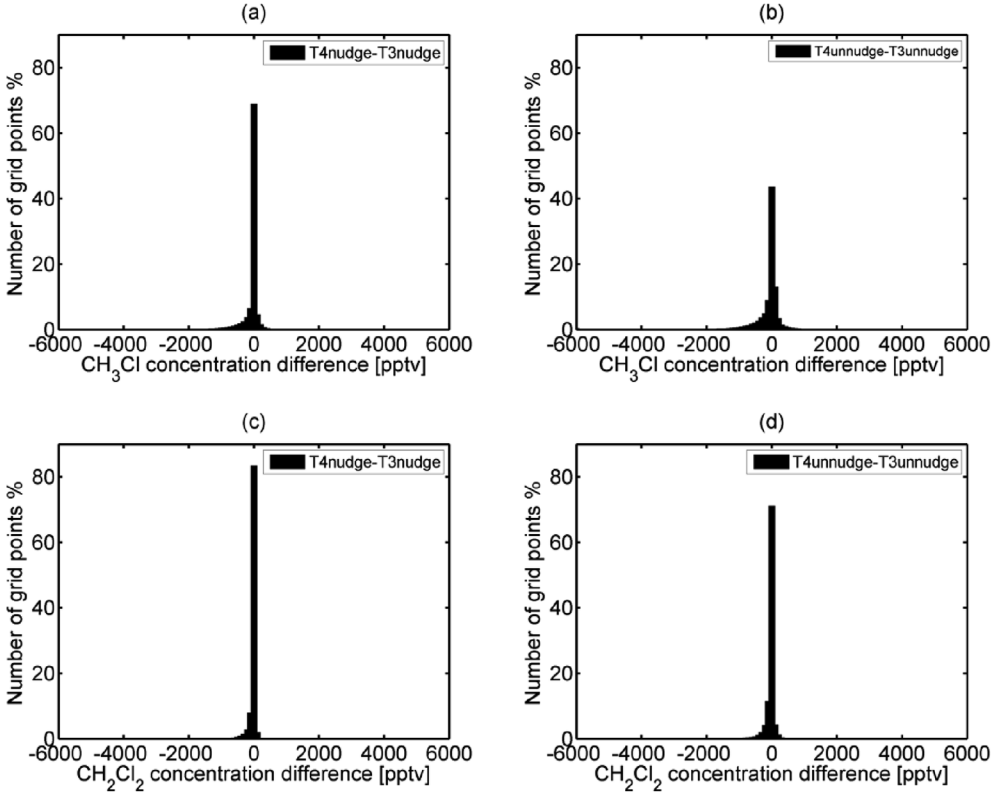

Fig. 14. Frequency distribution of Chloromethane, CH_2Cl_2 concentration difference of different emission function with constant meteorology.

Table 3
Calculated global emission of CH_3Cl and CH_2Cl_2 from the mangrove forest.

Tracers	$E^{measured}(1.3776 \times 10^5 km^2)$	$E^{measured}$ $(2 \times 10^5 km^2)$	Observatinal uncertainty (%)
$T3nCH_3Cl$	6 Gg yr^{-1}	9 Gg yr^{-1}	± 18 (1σ)
$T4nCH_3Cl$	5 Gg yr^{-1}	8 Gg yr^{-1}	± 18 (1σ)
$T3unCH_3Cl$	7 Gg yr^{-1}	10 Gg yr^{-1}	± 18 (1σ)
$T4unCH_3Cl$	4 Gg yr^{-1}	6 Gg yr^{-1}	± 18 (1σ)
$T3nCH_2Cl_2$	2 Gg yr^{-1}	2 Gg yr^{-1}	± 18 (1σ)
$T4nCH_2Cl_2$	1 Gg yr^{-1}	2 Gg yr^{-1}	± 18 (1σ)
$T3unCH_2Cl_2$	2 Gg yr^{-1}	3 Gg yr^{-1}	± 18 (1σ)
$T4unCH_2Cl_2$	1 Gg yr^{-1}	2 Gg yr^{-1}	± 18 (1σ)

global mangrove area. This bottom-up approach is also commonly used in emission inventories for anthropogenic emissions. We present the up-scaled emission of CH_3Cl, CH_2Cl_2 using the model results and observations in the mangrove forest region. From equation (4) one can calculate the measured emission using the ratio of concentartion differences between upwind and downwind from the model to the observed values. The local emissions are represented as gram per square meter per second for different passive tracers. These scaled local emissions were then used to upscale to global emissions of mangroves.

The global mangrove area is slightly reduced at present (Giri et al., 2011) compared to the previous study by Duarte et al. (2005). Manley et al. (2007) used laboratory measurements of a single grown mangrove in a green house experiment data to up-scale the CH_3Cl contribution. Using a global area of 2×10^5 km^2, they estimated a CH_3Cl emission of 12 Gg yr^{-1}. In the present study the average CH_3Cl global mangrove emission using different emission functions and with different meteorology yielded 4–7 Gg yr^{-1} and 6–10 Gg yr^{-1} for the updated mangrove area and the previously quantified area, respectively (Table 3).

Our estimated values are thus lower to slightly lower than the laboratory measurements by Manley et al. (2007). This suggests that we estimate a little less emission than the laboratory study. Using the CH_3Cl global sink strength of 4106 Gg yr^{-1} (WMO, 2010), the estimated range of mangrove production in the present study is 0.2 percent to 0.3 percent (global mangrove area of 2×10^5 km^2). The estimated range of mangrove production is 0.1 percent to 0.2 percent assuming a newly available global mangrove area of 1.3776×10^5 km^2. The observational error in the concentration is about ± 9 percent. The maximum observational error in the mangrove emission is about ± 18 percent using the gradient method.

The estimated CH_2Cl_2 global mangrove contribution is in the range of 1–2 Gg yr^{-1} using the updated mangrove area 2–3 Gg yr^{-1} for the older estimate for mangrove areas. We do not have any other observed values of CH_2Cl_2 emission from mangroves from the literature. It has been concluded that mangroves emit CH_2Cl_2 as well. Since the value for CH_3Cl is a reasonable range one might assume that this new value for CH_2Cl_2 might also be reliable. The estimated annual emission of CH_2Cl_2 from the industrial sources, biomass burning and oceans is 604 ± 251 Gg yr^{-1} (Keene, 1999). Similarly Xiao (2008) estimated annual emission of CH_2Cl_2 at 629 ± 44 Gg yr^{-1}. Based on the present study the mangroves contribute 0.03 percent of CH_2Cl_2 in the global emission budget.

4. Conclusion

This study presents the first field measurements from the tropical Braganca mangrove ecosystem. We also study the transport of concentrations of CH_3Cl, CH_2Cl_2 across the mangrove source region. A simple Lagrangian approach has been used in this study. This approach may since be recommended for field studies in the forest region if the observations are intended to collect continuously.

We also present the impact of meteorology on the dispersion of halocarbons represented as passive tracers. In order to understand the impact of meteorology on concentrations, we conducted two experiments with the METRAS mesoscale model. One experiment is METRAS driven by the large-scale forcing of the MBAR model (nudge meteorology case). Another simulation is without any large-scale forcing (unnudge meteorology case) of meteorology in METRAS. The model simulated concentrations are then normalized using the observed CH_3Cl and CH_2Cl_2 concentration in the mangrove forest region.

The concentration difference between upwind and downwind is 744 pptv for CH_3Cl. In the case of CH_2Cl_2 the difference is 178 pptv. The calculated concentration gradient is 93 pptv per km for CH_3Cl. In the case of CH_2Cl_2 the concentration gradient is 22 pptv per km from the mangrove forest. The calculated gradient and concentration difference may suggest that mangroves emit CH_3Cl as well as CH_2Cl_2.

In the case of the mangrove source region, meteorology has shown a larger impact on concentrations than the different emission functions used in METRAS. Emission functions do show a little influence in the concentrations.

The combination of measured air concentrations and simulated tracer transport with different types of emission functions allows the calculation of CH_3Cl and CH_2Cl_2 emissions and, thus, an estimation of the source strength from mangrove forests.

The mean annual emission of CH_3Cl, CH_2Cl_2 using different emission functions with different meteorology are 6–10 Gg yr^{-1} for CH_3Cl and 2–3 Gg yr^{-1} for CH_2Cl_2 using the larger mangrove area as used in previous estimates.

Acknowledgments

This work is supported through the cluster of Excellence 'CliSAP' (EXC177), University of Hamburg, funded through the Deutsche Forschungsgemeinschaft. The authors thank F. Laturns for sampling and E. Bahlmann for reviewing concentration data. We also thank Prof. Dr. Nils Edvin Asp for sharing his lab and help during the field work in Braganca, Brazil. The authors would like to thank INMET for providing MBAR model forecast data. We thank the two anonymous reviewers and editor for their comments on our manuscript.

References

Alongi, D., 2002. Present state and future of the worlds mangrove forests. Environ. Conserv. 29, 331–349.
Bahlmann, E., Weinberg, I., Seifert, R., Tubbesing, C., Michaelis, W., 2011. A high volume sampling system for isotope determination of volatile halocarbons and hydrocarbons. Atmos. Meas. Tech. 4, 2073–2086.
Blei, E., Hardacre, C.J., Mills, G.P., Heal, K.V., Heal, M.R., 2010. Identification and quantification of methyl halide sources in a lowland tropical rainforest. Atmos. Environ. 44, 1005–1010.
Butler, J.H., 2000. Atmospheric chemistry better budgets for methyl halides? Nature 403, 260–261.
Dierer, S., Schlünzen, K.H., Birnbaum, G., Brümmer, B., Müller, G., 2005. Atmosphere-sea ice interactions during a cyclone passage investigated by using model simulations and measurements. Mon. Weather Rev. 133, 3678–3692.
Duarte, C.M., Middelburg, J.J., Caraco, N., 2005. Major role of marine vegetation on the oceanic carbon cycle. Biogeosciences 2, 1–8.
Duke, N.C., Meynecke, J.O., Dittmann, S., Ellison, A.M., Anger, K., Berger, U., Dahdouh-Guebas, F., 2007. A world without mangroves? Science 317, 41–42.
Ellison, A.M., Farnsworth, E.J., 2001. Mangrove communities. In: Bertness, M.D., Gaines, S.D., Hay, M.E. (Eds.), Marine Community Ecology. Sinauer, Sunderland, pp. 423–442.
Giri, C., Ochieng, E., Tieszen, L.L., Zhu, Z., Singh, A., Loveland, T., Masek, J., Duke, N., 2011. Status and distribution of mangrove forests of the world using earth observation satellite data. Glob. Ecol. Biogeogr. 11, 154–159.
Harper, D., 1985. Halomethane from halide iona highly efficient fungal conversion of environmental significance. Nature 315, 55–57.
Hogarth, P., 1999. The Biology of Mangroves. Oxford Univ. Press, New York.
Kaiser, J.W., Heil, A., Andreae, M.O., Benedetti, A., Chubarova, N., Jones, L., Morcrette, J.-J., Razinger, M., Schultz, M.G., Suttie, M., van der Werf, G.R., 2012. Biomass burning emissions estimated with a global fire assimilation system basedon observed fire radiative power. Biogeosciences 9, 527–554.
Kathiresan, K., Bingham, B.L., 2001. Biology of mangroves and mangrove ecosystems. In: In: A. J. S (Ed.), Advances in Marine Biology, vol. 40. Elsevier, New York, pp. 81–251.
Keene, W. C. e. a, 1999. Composite global emissions of reactive chlorine from

anthropogenic and natural sources: reactive chlorine emissions inventory. J. Geophys. Res. 104 (D7), 8429–8440.
Khalil, M.A.K., Rasmussen, R.A., 1999. Atmospheric methyl chloride. Atmos. Environ. 33, 1305–1321.
Kolusu, S., Schlünzen, K.H., Grawe, D., Seifert, R., 2017. Chloromethane and dichloromethane in the tropical Atlantic Ocean. Atmos. Environ. 150, 417–424.
Kolusu, S.R., 2013. Determination of Methyl Halide Emissions from Measurements and Mesoscale Atmospheric Model Simulations. Phd thesis. Dep. of Earth Sciences., Univ. of Hamburg, Hamburg, Germany.
Kolusu, S.R., Marsham, J.H., Mulcahy, J., Johnson, B., Dunning, C., Bush, M., Spracklen, D.V., 2015. Impacts of amazonia biomass burning aerosols assessed from short-range weather forecasts. Atmos. Chem. Phys. 15, 12251–12266.
Lee-Taylor, J., Doney, S., Brasseur, G., Muller, J.-F., 1998. A preliminary three-dimensional global model study of atmospheric methyl chloride distributions. J. Geophys. Res. 16039–16057.
Lobert, J.M., Keene, W.C., Logan, J.A., Yevich, R., 1999. Global chlorine emissions from biomass burning: reactive chlorine emissions inventory. J. Geophys. Res. 104, 8373–8389.
Lüpkes, C., Schlünzen, K.H., 1996. Modelling the arctic convective boundary-layer with different turbulence parameterizations. Boundary-Layer Meteorol. 79, 107–130.
Majewski, D., Frank, H., Liermann, D., 2010. Gme userś guide version 2.23, corresponding to model version gmtri 2.23 and higher. dwd. Offenbach, 72.
Manley, S.L., Wang, N.-Y., Walser, M.L., Cicerone, R.J., 2007. Methyl halide emissions from greenhouse-grown mangroves. Geophys. Res. Lett. 34, L01806.
Marlier, M.E., DeFries, S.R., Voulgarakis, A., Kinney, P.L., Randerson, J.T., Shindell, D.T., Chen, Y., Faluvegi, G., 2013. El nino and health risks from landscape fire emissions in southeast asia. Nat. Clim. Change 3, 131–136.
Moore, R., Groszko, W., Niven, S., 1996. Ocean-atmosphere exchange of methyl chloride: results from nw atlantic and pacific ocean studies. J. Geophys. Res. 101, 28529–28538.
Niemeier, U., Schlünzen, K.H., 1993. Modelling steep terrain influences on flow patterns at the isle of helgoland. Beiträge zur Phys. Atmosphäre 66, 45–62.
Polidoro, B.A., Carpenter, K.E., Collins, L., Duke, N.C., Ellison, A.M., et al., 2010. The loss of species: mangrove extinction risk and geographic areas of global concern. PLoS One 5 (4), e10095. http://dx.doi.org/10.1371/journal.pone.0010095.
Rayner, N.A., Parker, D.E., Horton, E.B., Folland, C.K., Alexander, L.V., Rowell, D.P., Kent, E.C., Kaplan, A., 2003. Global analyses of sea surface temperature, sea ice, and night marine air temperature since the late nineteenth century. J. Geophys. Res. 108, 4407. http://dx.doi.org/10.1029/2002JD002670 D14.
Rhew, R., Miller, B., Weiss, R., 2000. Natural methyl bromide and methyl chloride emissions from coastal salt marshes. Nature 292–295.
Schlünzen, K.H., Flagg, D.D., Fock, B.H., Gierisch, A., Lüpkes, C., Reinhardt, V., Spensberger, C., 2012. Scientific Documentation of the Multiscale Model System M-SYS (METRAS, MITRAS, MECTM, MICTM, MESIM) - Version: 2012-02-09, MEMI Technical Report4.
Schlünzen, K.H., Katzfey, J.J., 2003. Relevance of subgrid-scale land-use effects for mesoscale models. Tellus 55A, 232–246.
Schueler, S., Schlünzen, K.H., 2006. Modeling of oak pollen dispersal on the landscape level with a mesoscale atmospheric model. Environ. Model. Assess. 11, 179–194.
WMO, 2010. Global Ozone Research and Monitoring Project-report 52.
Xiao, X., 2008. Optimal Estimation of the Surface Fluxes of Chloromethanes Using a 3-d Global Atmospheric Chemical Transport Model. Phd thesis. MIT, Cambridge.
Yokouchi, Y., Ikeda, M., Inuzuka, Y., Yukawa, T., 2002. Strong emission of methyl chloride from tropical plants. Nature 416, 163–165.
Yokouchi, Y., Machida, T., Barrie, L., Toom-Sauntry, D., Nojiri, Y., Fujinuma, Y., Inuzuka, Y., Li, H.-J., Akimoto, H., Aoki, S., 2000a. Latitudinal distribution of atmospheric methyl bromide: measurements and modelling. Geophys. Res. Lett. 27, 697–700.
Yokouchi, Y., Nojiri, Y., Barrie, L., Toom-Sauntry, D., Machida, T., Inuzuka, Y., Akimoto, H., Li, H.-J., Fujinuma, Y., Aoki, S., 2000b. A strong source of methyl chloride to the atmosphere from tropical coastal land. Nature 403, 295–298.